

WOOD HEMICELLULOSE/CHITOSAN-BASED SEMI-INTERPENETRATING NETWORK HYDROGELS: MECHANICAL, SWELLING AND CONTROLLED DRUG RELEASE PROPERTIES

Ahmet M. Karaaslan,^a Mandla A. Tshabalala,^b and Gisela Buschle-Diller^{a*}

The cell wall of most plant biomass from forest and agricultural resources consists of three major polymers, cellulose, hemicellulose, and lignin. Of these, hemicelluloses have gained increasing attention as sustainable raw materials. In this study, novel pH-sensitive semi-IPN hydrogels based on hemicelluloses and chitosan were prepared using glutaraldehyde as the crosslinking agent. The hemicellulose isolated from aspen was analyzed for sugar content by HPLC, and its molecular weight distribution was determined by high performance size exclusion chromatography. Results revealed that hemicellulose had a broad molecular weight distribution with a fair amount of polymeric units, together with xylose, arabinose, and glucose. The effects of hemicellulose content on mechanical properties and swelling behavior of hydrogels were investigated. The semi-IPNs hydrogel structure was confirmed by FT-IR, X-ray study, and the ninhydrin assay method. X-ray analysis showed that higher hemicellulose contents yielded higher crystallinity. Mechanical properties were mainly dependent on the crosslink density and average molecular weight between crosslinks. Swelling ratios increased with increasing hemicellulose content and were high at low pH values due to repulsion between similarly charged groups. *In vitro* release study of a model drug showed that these semi-IPN hydrogels could be used for controlled drug delivery into gastric fluid.

Keywords: Hemicellulose; Forest biomass; Hydrogel; Film; Semi-IPN; Chitosan; pH-sensitive; Drug release; Interpenetrating network

Contact information: a: Department of Polymer and Fiber Engineering, Auburn University, Auburn, Alabama 36849-5327; b: USDA Forest Products Laboratory, One Gifford Pinchot Drive Madison Wisconsin 53726, *Corresponding author: buschgi@auburn.edu

INTRODUCTION

Raw materials from renewable resources have gained increasing importance in recent years as fossil fuels become less available. Forest by-products from low-value trees, bark, and residue from sawmills offer an alternative as renewable resources. Products based on forest biomass find applications in areas where biocompatibility and biodegradability are of major importance. Careful extraction and fractionation of forest biomass can yield chemicals, which in turn can be converted into high-value products. An example of useful silvichemicals is hemicelluloses, a class of hetero-polysaccharides present in the cell wall of wood and annual plants together with cellulose and lignin (Timell 1967). Hemicellulose is considered to be the second most abundant polysaccharide in nature, representing about 20-35% of lignocellulosic biomass. Potential applications of hemicelluloses and their derivatives have been described in the literature

(Ebringerova 2006). One such area of application is super-absorbent hydrogels. Hydrogels have attracted significant attention in biological and biomedical applications based on their high liquid up-take, their stimuli-responsive swelling-deswelling capabilities without disintegration, and their biocompatibility (Peppas et al. 2006; Slaughter et al. 2009; Hoare and Kohane 2008). Hydrogels generally consist of three-dimensional hydrophilic polymeric networks. They owe their mechanical stability during swelling to chemical and/or physical cross-links between the macromolecular chains (Peppas et al. 2000) that allow for flexibility, yet render low, but sufficient strength. Polysaccharides such as chitosan and alginate have been widely used to prepare natural hydrogels that have the advantages of biocompatibility, biodegradability, low toxicity, and availability from renewable resources (Coviello et al. 2007).

Efforts have been made to improve their mechanical properties without impairing their sorption capabilities. Reinforcement with small fibers, formation into nanocomposites, chemical crosslinking and formation of interpenetrating (IPN) or double networks are some of the strategies that have been employed (Tanaka et al. 2005; Schexnailder and Schmidt 2009; Myung et al. 2008). Of those, semi-interpenetrating network hydrogels (semi-IPNs) have been extensively described (Liu et al. 2010; Jin et al. 2006; Zhao et al. 2006). Semi-IPNs are achieved by blending two polymers with one being crosslinked in the presence of the other (not crosslinked) polymer (Čulin et al. 2005). In semi-IPNs, additional interactions between the two polymers such as hydrogen bonds, crystallites, ionic, and hydrophobic interactions may participate in the hydrogel formation (Berger et al. 2004). Moreover, each polymer might contribute to the final properties of semi-IPN hydrogels in terms of mechanical stability (Zugic et al. 2009), stimuli responsiveness to pH (Zhang et al. 2005), and temperature (Gua and Gao 2007).

Recent studies showed that agricultural and forestry by-products can also be incorporated into hydrogels. In this context, hemicelluloses have been explored by some research groups (Gabriellii and Gatenholm 1998; Gabriellii et al. 2000; Lindblad et al. 2001, 2005). Gabriellii et al. (2000), for example, studied chitosan hydrogels that contained xylan for reinforcement. They concluded that crystalline arrangement and electrostatic interactions between two biopolymers were responsible for the relatively high stability of the hydrogels.

Chitosan is a cationic polysaccharide known for its good film forming ability. It is obtained from waste chitin, and as such can be considered a material from renewable resources. Amine groups attached to its backbone enable chitosan to become positively charged in acidic medium. Therefore, chitosan can serve as a biomaterial for pH-responsive hydrogel applications. However, these hydrogels generally lack mechanical stability unless they are crosslinked and/or reinforced by suitable compounds.

In this study, hemicelluloses isolated from aspen were evaluated for use as value-added biomaterials. For this purpose, novel semi-IPN hydrogels based on hemicellulose and chitosan were prepared and designed for application in pH-responsive drug delivery systems by using riboflavin as the model active agent. It has been hypothesized that alkaline extracted hemicellulose could be entrapped in a chemically crosslinked pH-responsive polymer network such as chitosan. If the hemicellulose was capable of crystallizing, it would act as a reinforcing component for enhancing the mechanical

properties of this semi-IPN hydrogel. It is further hypothesized that such a semi-IPN hydrogel could be constituted into a potential controlled release drug delivery system.

EXPERIMENTAL

Materials

Chitosan with 190,000-310,000 g/mol viscosity average molecular weight and 75-85% degree of deacetylation was obtained from Sigma Aldrich. Glutaraldehyde, acetic acid, riboflavin, and other solvents and chemicals were purchased from Fisher Scientific and used as received. For comparison, experiments with commercially available xylan from birch wood of known chemical composition (Sigma Aldrich) were also performed.

Isolation of Hemicelluloses from Wood Flour

Hemicellulose, isolated from aspen by a novel alkaline extraction method, was provided by USDA Forest Products Laboratory, Madison, WI. Aspen chips were processed into flour in a Wiley mill to pass through a 1-mm mesh size screen attached to the mill. The flour was sieved on a 60-mesh screen. Fifty (50) grams of the fraction captured on the 60-mesh screen was treated with 500 mL 0.05 M HCl at 70°C for 2 h. The suspension was allowed to cool to room temperature before adjusting its pH to 9.2 with approximately 6 mL concentrated NH₄OH. The suspension was stirred overnight at room temperature and filtered under suction on Whatman GF/A glass microfiber filter paper to extract pectins, starch, and fats. The filter cake was placed in 500 mL 0.025M NaOH in 70% ethanol at 75°C and stirred for 2 h to solubilize lignin. The suspension was allowed to cool to room temperature before filtration under suction on Whatman GF/A glass microfiber filter paper to remove lignin. The remaining filter cake was transferred to 500 mL 0.1M NaOH, and stirred for 16 h at room temperature to solubilize hemicelluloses. At the end of this period the suspension was filtered under suction on Whatman GF/A glass microfiber filter paper, to isolate hemicelluloses in the filtrate. The filtrate was heated to 65°C, and 35 mL 30% H₂O₂ was added to the filtrate in 1-mL increments and it was allowed to react under constant stirring. When the filtrate had turned white, it was allowed to cool to room temperature. Its pH was adjusted to 5.3 with 32 mL concentrated HCl before transferring it to three-times its volume of 95% ethanol. The mixture was left overnight to allow hemicellulose to precipitate. The supernatant liquid was carefully removed by vacuum suction, and the hemicellulose precipitate was reconstituted in 300-500 mL of reverse osmosis (RO) water. This hemicellulose solution was dialyzed in a Spectra/Por dialysis membrane, MWCO: 3500, against 3000 mL RO water. After overnight dialysis, the dialyzed hemicellulose solution was freeze-dried to yield hemicellulose powder. A sample of the hemicellulose powder was dissolved in 0.1M NaNO₃ for molecular weight determination by high performance size exclusion chromatography with refractive index (HPSEC-RI) and UV (HPSEC-UV) detection. Another sample of the hemicellulose powder was hydrolyzed, and the hydrolysate was analyzed for sugar content by HPLC with electrochemical detection (HPLC-ED).

Hydrogel Preparation

Chitosan was dissolved in 2% v/v acetic acid aqueous solution to prepare 1% w/w chitosan solution. Hemicellulose was added to deionized water at 1% w/v and heated to 95°C for 20 minutes with stirring. The solution was cooled to room temperature. Blended hydrogels were prepared by mixing chitosan and hemicellulose solution for 8 h at 70:30 and 30:70 weight ratios with a total dry matter of 1%.

For crosslinking, glutaraldehyde was added at a set ratio (3% w/w) to the total dry weight of chitosan in the solution after stirring the mixtures for 8 h. Final solutions were cast into films in plastic petri dishes and dried in an oven at 40°C for 24 h. The dry films were immersed in 0.1 N sodium hydroxide solution to neutralize acetic acid residues, then washed with ethanol to remove an excess NaOH. After rinsing with excess deionized water, the films were dried in an oven at 40°C for 24 h. The average crosslink density of samples reported in this paper was determined to be 22% unless otherwise noted. FT-IR spectra of crosslinked chitosan films did not show any traces of unreacted glutaraldehyde.

Hydrogel Characterization

Crosslinking density

The effective crosslink density was estimated using the kinetic theory of rubbery elasticity (Eq. 1; Yui 2002; Ma and Elisseff 2005; Lou and Copenhagen 2001),

$$G = RT\nu_e\nu_2^{1/3} \quad (1)$$

where G is the elastic modulus, ν_e is the effective crosslink density, ν_2 is the polymer volume fraction at equilibrium swollen state, R is the gas constant, and T is the temperature in Kelvin. The elastic modulus of swollen hydrogels, G , was determined from the linear portion of the stress-strain curve at low strains by using Eq. 2,

$$\tau = G \left[\alpha - \frac{1}{\alpha^2} \right] \quad (2)$$

where τ is the force per unit of initial cross-sectional area of swollen gel and α is the deformation ratio (deformed length/initial length) of the network by tensile force.

The average molecular weight between crosslinks (\overline{M}_c , g/mol) was calculated as follows (Eq. 3:1, Yu et al. 2007):

$$\overline{M}_c = \frac{1}{\nu_e \bar{v}} \quad (3)$$

where ν_e is the effective crosslink density in mol/cm³ obtained by Eq.1, and \bar{v} is the specific volume of the polymer in cm³/g.

In addition, the degree of crosslinking was also determined by the percent decrease of free amine groups in the hydrogels. The ninhydrin assay method, which is commonly used for quantitative determination of free amine (NH₂) groups in chitosan

(Curotto and Aros 1993; Mi et al. 2001), was performed according to the standard procedure.

Mechanical Properties

The fiber-film geometry module of the RSAIII Dynamical Mechanical Analyzer with a 3.5 kg load cell was used to test the tensile properties of the dry hydrogel films. Crosshead speed and gauge length was 1 mm/min and 10 mm, respectively. Samples were cut into 7x30 mm strips. The thickness of the film sample was measured using a digital micrometer with 0.001 mm resolution at three locations and averaged. Samples were conditioned at 65% RH and 22°C for about 48 h before testing. Replicate tests of at least three films were performed.

Tensile testing of the swollen hydrogel films at equilibrium was performed with an Instron Universal Tester with a 100 N load cell. Gauge length and crosshead speed were set to 10 mm and 2 mm/min, respectively. Samples were cut into 7x30 mm strips before immersing in deionized water. In order not to damage the swollen samples during the thickness measurements, they were gently sandwiched between microscope cover slips. To prevent water loss during testing, hydrogel samples were coated with petroleum gel (Anseth et al. 1996).

Swelling Behavior

For the swelling experiments, dry films with an average thickness of 17 μm were cut into samples of 10 mm x 10 mm. Each sample weighed approximately 6 mg.

The equilibrium swelling ratio of hydrogels, which signifies the expanding and retracting forces between crosslinks at equilibrium, was determined by water uptake measurements. Pre-weighed dry samples were immersed in deionized water at room temperature for 1 h, which was determined to be sufficient to reach the equilibrium state. The weight of the swollen samples was measured after blotting excessive water gently with filter paper. The equilibrium swelling ratio (S) was calculated by the following equation (Eq. 4),

$$S(\%) = \frac{W_s - W_d}{W_d} \times 100 \quad (4)$$

where W_s and W_d are the swollen and dry weight of samples, respectively. Equilibrium swelling ratios at different pH buffers (2, 4, 6, 8, and 10) were determined as described above.

In vitro cumulative release study

In order to load the model drug into the hydrogels, riboflavin was added to chitosan/ hemicellulose solution before the crosslinking step. The amount of drug loaded was 20% (w/w) of total dry matter in the final solution. Solubility of riboflavin in DI water is low (<0.05%); however riboflavin is highly soluble in dilute alkaline solutions. To minimize the drug loss before the *in vitro* test, samples were immersed in DI water for 1 h, rinsed with excess water (without using sodium hydroxide and ethanol) and oven-dried. Drug loss from dried films was determined by measuring the absorbance of the

rinse water at 445 nm with UV-vis. The amount of drug loaded (M_0) before the *in vitro* test was calculated by subtracting the amount of drug loss from the initial amount of drug loaded.

To simulate the release of riboflavin into physiological media, riboflavin loaded hydrogels with the same dimensions as used for the swelling experiments were incubated in 25 mL pH 2.2 and pH 7.4 phosphate buffer solutions with same concentration (0.1 M) and ionic strength (0.1 M) at 37°C and shaken at 50 rpm. At different time intervals, 4 mL of test solution were extracted and 4 mL fresh buffer solution added. The concentration of riboflavin released was determined by measuring the absorbance at 445 nm with a UV-vis spectrophotometer. Cumulative release (M_t/M_0 , %) was determined by the ratio of the amount of drug released (M_t) at time t to the initial amount of drug loaded (M_0).

Structural and morphological analysis

FTIR spectra of dry films were obtained with a Nicolet 6700 FT-IR spectrometer between 4000 and 400 cm^{-1} over 32 scans with a resolution of 4 cm^{-1} .

The crystallinity of the films was analyzed using a Bruker D8 X-ray diffractometer. Cu $K\alpha$ radiation at 40 kV and 40 mA with a wavelength of 1.54 Å was used, and 2θ was varied between 5 and 30° at a rate of 2° per min and a step size of 0.01°. The degree of crystallinity (ϕ , Eq. 5) was calculated by TOPAS software. The amorphous baseline was determined by a first order Chebyshev polynomial fit to the experimental diffractogram according to Rogers et al. (2005). The relationship of the intensity of amorphous background (ΣI_a) to the total intensity (ΣI_{exp}) was then calculated to yield the degree of crystallinity as follows:

$$\phi = \left(1 - \frac{\Sigma I_a}{\Sigma I_{exp}}\right) \times 100 \quad (5)$$

The surface morphology of films was examined by a Zeiss EVO 50 scanning electron microscope (SEM) at 15 kV. Samples were sputter-coated with gold prior to examination. The appearance of the films was also evaluated by a Nikon SMZ-U optical light microscope with 10x zoom.

RESULTS AND DISCUSSION

Hemicellulose Extraction

Sugar analysis of hemicellulose fractions (see Table 1) from aspen wood showed that the fraction most suitable for hydrogel formation experiments contained mostly xylose (82%), arabinose (8%) and glucose (5%). For comparison, a commercially available xylan sample from birch wood was also hydrolyzed and analyzed for sugars. It was found to contain less xylose (75%) and glucose (1%) and basically no arabinose.

Table 1. Sugar Composition of Hydrolysates of Hemicellulose Fractions and Commercial Xylan (%)

	Arab	Gal	Rham	Glc	Xyl	Man	Residue	Total CHO
Hemicellulose	8.2	2.2	0.0	5.1	82.1	2.4	0.0	100.0
Commercial xylan	-	0.4	0.0	1.02	75.3	-	-	76.9

Size exclusion chromatography results revealed a fairly broad molecular weight distribution with large amounts of low and medium molecular weight, but also a fair amount of polymeric saccharides. Two peaks, detected by HPSEC-RI, and identified as Peak #1 and Peak #2 in Fig. 1, showed apparent molecular weights of $MW_p \approx 401,000$ and $391,000 \text{ g}\cdot\text{mol}^{-1}$, respectively. The observed polydispersity, however, is not unusual for hemicellulose extracted from forest biomass.

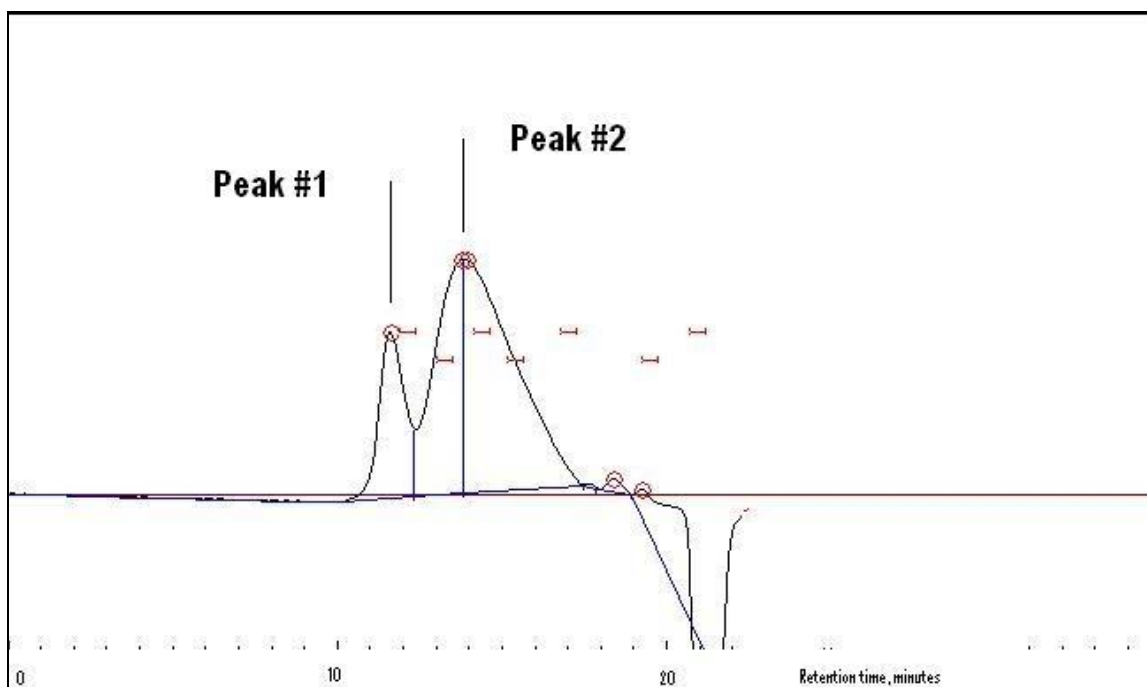


Fig.1. HPSEC-RI chromatogram of hemicellulose fraction: Peak #1 at retention time 11.5 min corresponds to $MW_p \approx 401,000 \text{ g}\cdot\text{mol}^{-1}$, and Peak #2 at retention time 13.8 min corresponds to $MW_p \approx 391,000 \text{ g}\cdot\text{mol}^{-1}$.

Although the chemical structure of the polysaccharides has not yet been determined in detail, it is reasonable to assume that the hemicellulose isolation procedure described in this paper yielded xylan-rich heteropolysaccharides with arabino-, gluco-, galacto-, and mannan- residues with some UV-absorbing moieties such as acetyl groups. The carboxyl group ($-\text{COOH}$) content was determined to be 0.01-0.02 mmol/g, which suggested the presence of $-\text{COOH}$ carrying glucuronic acid residues.

Teleman et al. (2000) performed extensive spectroscopic studies on hemicelluloses isolated from milled aspen chips and fractionated into oligomeric and polymeric components consisting mainly of O-acetyl-(4-O-methylglucurono)xylan.

According to their research, the backbone of this structure is constituted of β -(1 \rightarrow 4)-linked d-xylopyranosyl residues, substituted with one α -(1 \rightarrow 2)-linked 4-O-methyl-d-glucuronic acid per approximately every tenth such residue.

Film Formation

It was possible to cast films from aqueous solutions of hemicellulose on glass plates. However, the films were highly brittle with very low mechanical stability. Groendahl et al. (2004) argued that the poor film-forming ability and brittleness of glucuronoxylans is a direct consequence of insufficient chain length of the polymer, high glass transition temperature and poor solubility. Glucuronoxylan in its native state is amorphous but can crystallize to a certain extent after alkaline treatment due to partial removal of acetyl groups (Groendahl et al. 2004; Dimitriu 2004). The hemicellulose used in this study showed highly regular crystal formation when cast on glass plates from 1% w/v aqueous solutions. Figure 2 shows SEM micrographs of the observed highly regular crystallites. It is interesting to note that the commercial birch xylan could not be developed into films or flakes and did not demonstrate such crystal formations.

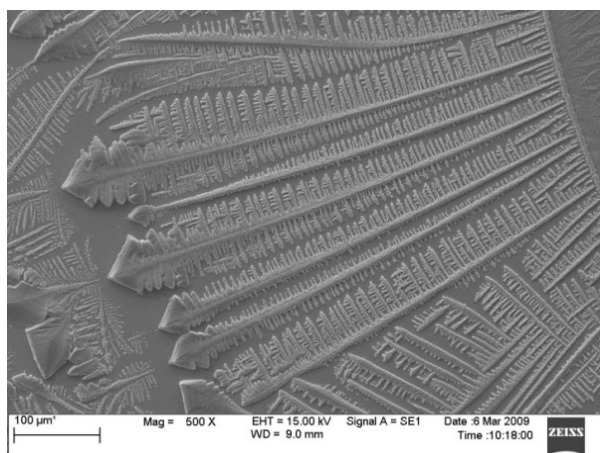


Fig. 2. SEM images of macroscopic crystal formation in 1% (w/v) aqueous hemicellulose solutions cast on glass plates.

Chitosan, as an extensively studied polysaccharide due its non-toxicity and biocompatibility, has been demonstrated to have excellent film-formation ability (Kumar et al. 2004). As expected, the mechanical stability of the hemicellulose films improved with using chitosan as the supporting matrix. At a ratio of 70:30 hemicellulose to chitosan, stable films were produced that showed spherulite formation (Fig. 3a) similar to those of hemicellulose samples without chitosan. With increasing chitosan content however, the form and size of the crystallites changed (Fig. 3b). At a ratio of 50:50 hemicellulose to chitosan, crystallite domains no longer overlapped, but rather showed space in-between separate domains without any interference.

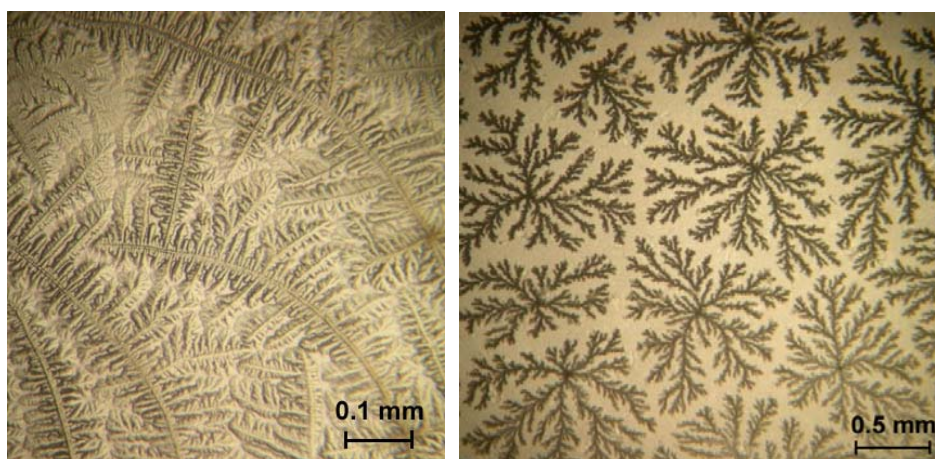


Fig. 3. Optical microscopic images of the dendritic crystals formed in hemicellulose/chitosan films; (a) H:CS = 70:30 (left-hand side), (b) H:CS = 50:50 (right-hand side).

At first, it was assumed that the crystallites primarily originated from the mono- or oligomeric components of hemicellulose. In this case these compounds would be removed upon exposure to repeated swelling/deswelling in distilled water. However, though less pronounced, crystallites similar to those shown in Fig. 3 were repeatedly formed.

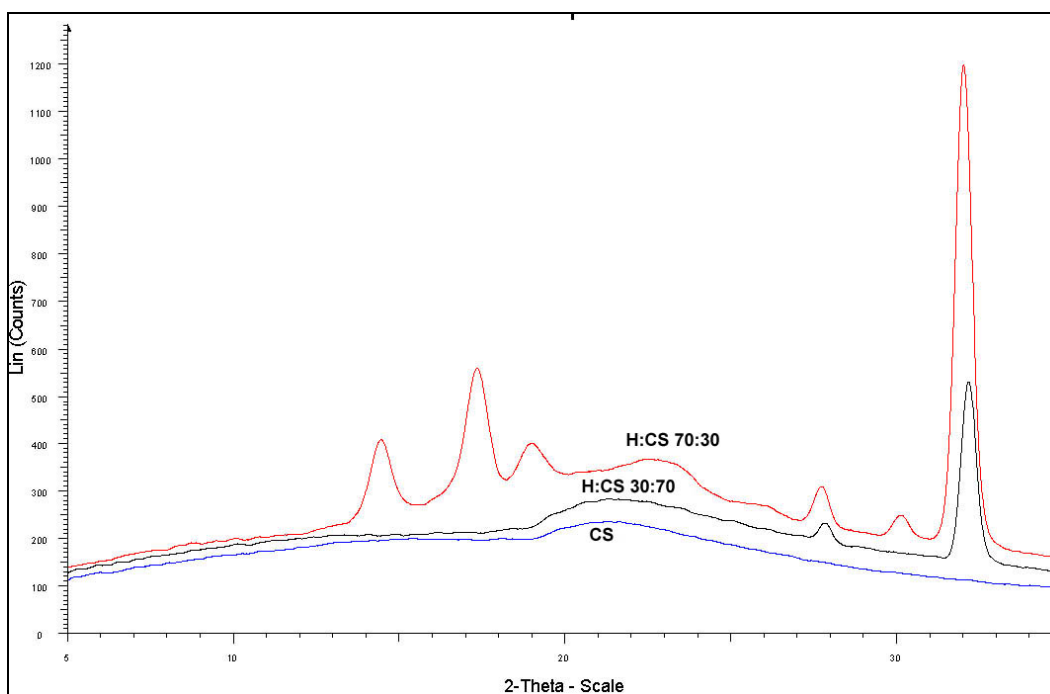


Fig. 4. X-ray diffractograms of films before swelling-deswelling cycles (CS; CS:H 70:30; CS:H 30:70).

Figure 4 shows X-ray diffractograms of hemicellulose/chitosan films before swelling in water as well as of films from chitosan without hemicellulose for comparison.

Clearly, higher hemicellulose contents yielded higher crystallinity. Major peaks were located at $2\theta=14.1$, 16.9, and 18.6, as found for hemicellulose. After swelling/deswelling, the crystallinity index of dry hydrogels was estimated to be 20.2% and 14.5% for 70:30 and 30:70 ratios of hemicellulose:chitosan, respectively. These results confirmed that the chitosan gel was able to entrap the crystallized water-insoluble polymeric portion of hemicellulose.

Semi-IPN Formation

By crosslinking of chitosan in presence of hemicellulose, a semi-interpenetrating network (IPN) structure could be formed. Semi-IPN formation was confirmed by FTIR, X-ray diffraction and the ninhydrin assay method. Figure 5 presents the FTIR spectra of hemicellulose, crosslinked chitosan, and semi-IPN hydrogel film at 30:70 hemicellulose:chitosan ratio. The peak at 1637 cm^{-1} can be attributed to the imine bond (C=N stretching) in the semi-IPN due to the Schiff's base reaction between chitosan and glutaraldehyde (Wang et al. 2004; Guan et al. 1996). A decrease in the percentage of free amine groups was also confirmed by ninhydrin assay (see Table 2). In comparison to crosslinked chitosan without hemicellulose, peak shifts were detected in the semi-IPN at 1540 cm^{-1} (NH deformation-amide II) and 3400 cm^{-1} (OH/NH stretching). These band shifts could be attributed to intermolecular interactions between hemicellulose and chitosan such as H-bonding and hydrophobic attraction. In addition, as proposed by Gabrielli et al. (1998 and 2000), some ionic interaction between carboxyl groups in hemicellulose and free amino groups in chitosan may also occur, although the amounts of carboxyl groups in hemicellulose are quite low (see Table 2).

Although some of the dendritic crystals shown in Fig. 3 were removed during rinsing and neutralization steps, X-ray diffraction measurements showed that a crystallinity of 14.5% and 20.2% for H:CS 30:70 and 70:30, respectively, had been preserved. Taking the ionic and intermolecular interactions as well as crystallinity introduced by hemicellulose chains into account, the structure of the crosslinked H:CS semi-IPN hydrogel could be proposed as schematically presented in Fig. 6. Interspersed crystalline regions and chemical crosslinks form the major support of the structure, while additional weaker interactions also contribute to the mechanical stability of the hydrogel.

Table 2. Amount of Carboxyl Groups in Hemicellulose

	Carboxyl groups (mmol/g)	Free amino groups (mmol/g)
Hemicellulose	0.01-0.02	-
Commercial xylan	0.05-0.06	-
Chitosan	-	2.05**
Chitosan***	-	1.60**

** averages determined by ninhydrin assay method described in experimental methods
 ***crosslinked with 3% w/w glutaraldehyde, degree of crosslinking was ~22%.

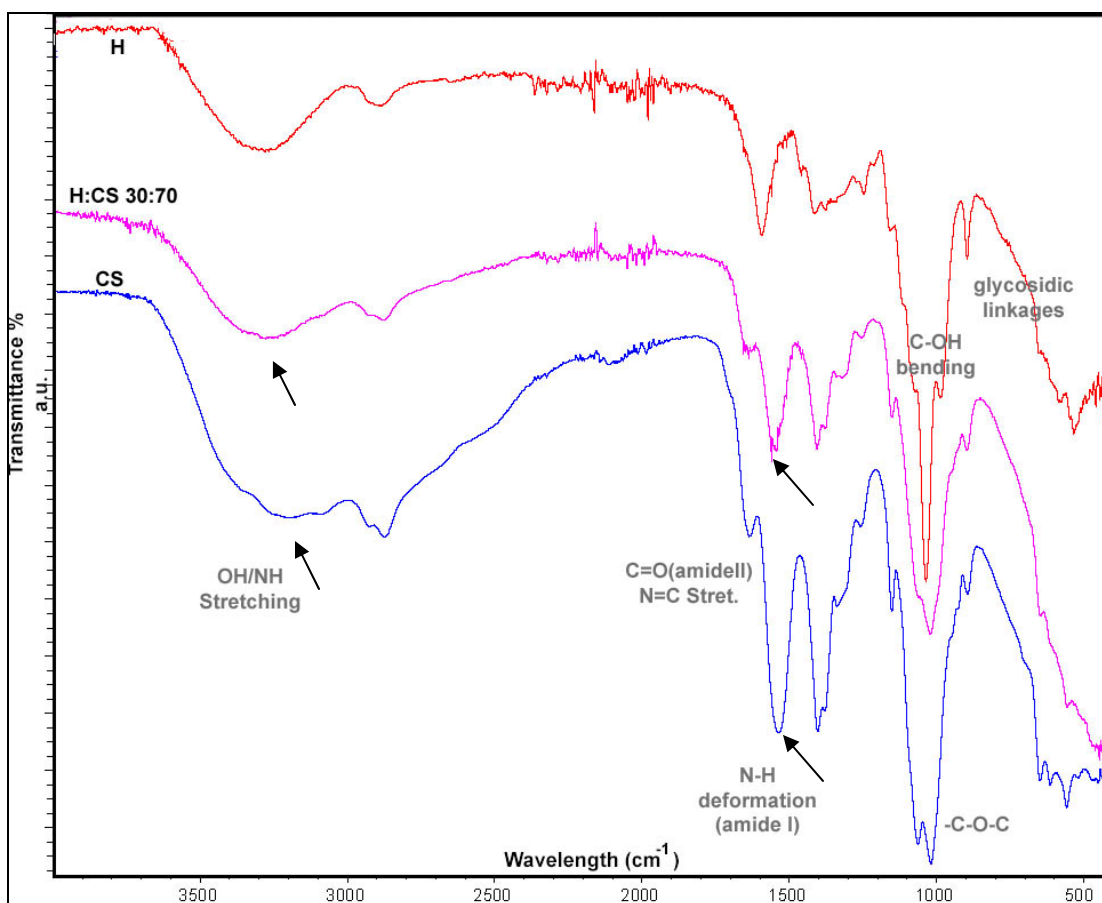


Fig. 5. FTIR spectra of dry hydrogel films with different hemicellulose compositions (arrows point at shifted peaks).

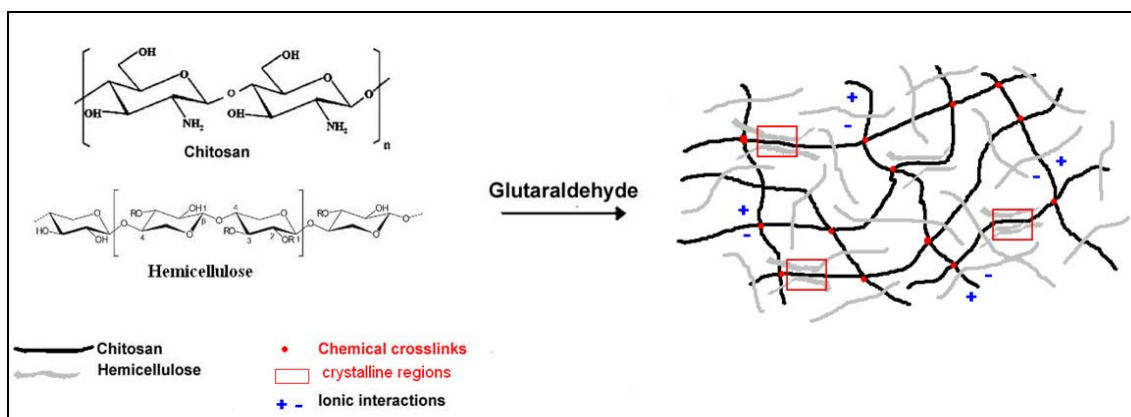


Fig. 6. Possible semi-interpenetrating network of crosslinked chitosan and entrapped hemicellulose with weak interactions to chitosan.

Mechanical Properties Hydrogel Films

The gelling properties of chitosan are well-documented (Berger et al. 2004). However chitosan gels without chemical or ionic crosslinks cannot be considered for

controlled drug delivery due to low mechanical stability in the swollen state. In this study, it was hypothesized that the addition of hemicellulose might have a sufficiently high stabilizing effect due to the introduction of crystallites and the interaction between the functional groups of hemicellulose and chitosan.

The mean and standard deviation values of Young's modulus, ultimate strength and strain to failure (standard deviations in brackets) are given in Table 3. Dry and water-swollen hemicellulose films without admixture of chitosan were too brittle to test. In the dry state of the films, hemicellulose did not enhance their mechanical properties, and crosslinked chitosan films were clearly stronger. However, in the swollen state the difference in strength between pure chitosan and chitosan/hemicellulose semi-IPN films was less. Absorbed water acted as a plasticizer and reduced the strength and modulus of swollen semi-IPN gels significantly, while slightly increasing the elongation. Strain to failure values were lower in both the swollen and dry state with increasing hemicellulose content. This might be attributed to the higher crystallinity of the semi-IPN films in comparison to the purely amorphous chitosan matrix. On the other hand, the crystallites formed in H:CS films showed little overlap, if at all (see Fig. 3). Instead, more or less isolated crystallites were observed.

Even though hemicellulose incorporation did not enhance the mechanical properties, observed values in regard to the tensile strength, Young's modulus and strain to failure for H:CS films in the dry state were comparable to those of biodegradable films reported in the literature (Hansen and Plackett, 2008). The similarity of mechanical properties of semi-IPN gels that contained hemicellulose and commercially available xylan showed that hemicellulose extracted for this study could compete with the products currently on the market.

Table 3. Mechanical Properties of Dry and Water-Swollen Hydrogel Films with Different Hemicellulose Compositions (standard deviations in brackets)

Films	Young's Modulus (MPa)	Ultimate Strength (MPa)	Strain to Failure (%)
H	Too brittle to test	Too brittle to test	Too brittle to test
H:CS 70:30-dry film	1390± 50	29.27±1.83	3.65±0.46
H:CS 30:70-dry film	2160±180	54.90±15.50	5.03±2.28
CS-dry film	2460±250	71.15±13.37	11.07±1.75
CS-swollen film	7.74± 1.01	1.46±0.32	23.15±4.51
H:CS 30:70-swollen film	4.79±0.21	0.46±0.23	12.67±4.74
X:CS 30:70-swollen film	5.33±1.08	0.45±0.08	11.23±1.37

It can be hypothesized that the decrease in modulus and strength values is a consequence of lower crosslink density and a simultaneous increase in average chain length between crosslinks (\overline{M}_c , g/mol) with hemicellulose inclusion into chitosan matrix (see Table 4). Effective crosslinking density was reduced from $4.6 \times 10^{-3} \text{ mol/cm}^3$ to $2.8 \times 10^{-3} \text{ mol/cm}^3$, while the average molecular weight of the chain length between crosslinks increased from 358 g/mol to 442 g/mol for semi-IPN gels with 30% hemicellulose content. The decrease in crosslink density and increase in \overline{M}_c may have

resulted in a more effortless movement of the chain segments within the network and thus led to a reduction in mechanical properties.

The crosslink density of H:CS 70:30 samples could not be determined because the tensile testing of these hydrogel films at swollen state was impossible. Even though these samples stayed intact in the swelling medium, samples were easily broken when taken out from the swelling medium for tensile testing.

Berger et al. (2004) suggested that an additional polymer whose hydrophilicity is different than chitosan might disturb the covalent crosslinking of chitosan chains, which then results in lower crosslink density. It is possible that glutaraldehyde formed fewer and/or longer crosslinks due to the strong intermolecular interactions between chitosan and hemicellulose. Although crystalline domains and additional secondary interactions were introduced with hemicellulose inclusion, it can be suggested that covalent crosslinks were the predominant factor that influenced the overall crosslinking density and resulted in lower modulus and strength.

Table 4. Crosslink Density and \overline{M}_c Values Calculated from Elastic Modulus of Swollen Hydrogels and Equilibrium Swelling Ratios in DI Water at Room Temperature

	Crosslink density (mol/cm ³)	\overline{M}_c (g/mol)	S (%)
CS	4.6± 0.5 x10 ⁻³	358±38	126±4
H:CS 30:70	2.8± 0.2 x10 ⁻³	442 ±32	136 ±13
H:CS 70:30	-	-	148±10

Swelling Behavior

The percentage equilibrium swelling ratios of semi-IPN hydrogels are listed in Table 4. As compared to crosslinked chitosan without hemicellulose, semi-IPN hydrogels had slightly higher swelling ratios with increasing hemicellulose content. Higher equilibrium swelling ratios can be attributed to lower crosslink density and higher \overline{M}_c (g/mol), which resulted in more space for water molecules.

It might have been expected that swelling ratios would be reduced with addition of hemicellulose into the chitosan matrix due to the formation of water-impermeable crystalline domains. Additionally, intermolecular interactions might be considered as physical crosslinks (Berger et al. 2004). However, as discussed previously, the reaction of glutaraldehyde could have been impaired by hemicellulose, and therefore higher swelling ratios were observed as a consequence of lower crosslink density and higher \overline{M}_c (g/mol).

pH-Dependant Swelling

According to Donnan equilibrium swelling theory, the osmotic pressure or ion concentration gradient between the inside and outside of a hydrogel is the driving force for swelling. If swelling/deswelling occurs in a narrow pH range and is caused by

ionization and repulsion of charged groups, the hydrogel is considered to be pH-sensitive. Such hydrogels are very useful as drug carriers.

The pH-dependant swelling behavior of CS and semi-IPN hydrogels at room temperature is shown in Fig. 7. At pH 4, the swelling ratios of semi-IPN hydrogels were fairly high. At pH 2, the observed slight decrease could be due to a shielding effect caused by excess H^+ . At basic pH values, swelling was clearly reduced, since the hydrogel contracted.

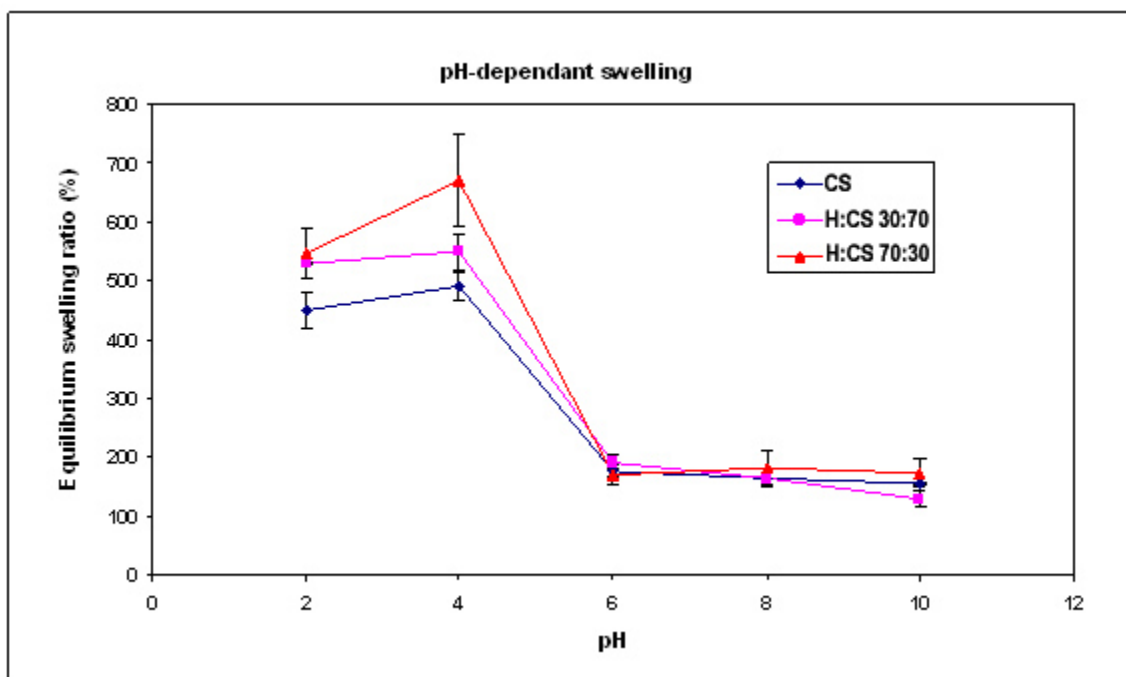


Fig. 7. Effect of pH on the swelling behavior of chitosan and hemicellulose/chitosan hydrogels determined at room temperature.

In Vitro Release Study

Release systems depend on the matrix, the drug to be discharged, and its solubility in both the matrix and the release medium. Riboflavin has been chosen as a model drug for this study due to its different solubility at different pH ranges and the aspect that it does not significantly interfere with the functional groups of the matrix. Due to the fact that it is not soluble under acidic conditions, the evaluation of the gel matrix becomes possible, separate from effects that occur due to drug solubility. Chitosan-based hydrogels have been reported for oral sustained delivery of antibiotics/ antiulcer drugs in the stomach (Shu et al. 2001). The semi-IPN gels reported in this study could be an alternative for this purpose.

At pH 2.2, the gel matrix was highly swollen (Fig. 7, room temperature), and the cumulative release of riboflavin from both CS and H:CS 70:30 gels was higher and faster than at pH 7.4 (Fig. 8). At this pH value, raising the temperature to 37°C caused an additional increase in equilibrium swelling ratio by 30% on the average. Therefore it was not surprising that within 3 h approximately 95% of the drug was released, although

riboflavin is little soluble at this pH. Therefore, it can be assumed that in this case riboflavin was discharged mainly as a consequence of the fairly open gel structure. The matrix most likely presented only a physical impediment for the release, and the interaction of riboflavin with release medium was of minor importance.

The total amount of riboflavin liberated at pH 7.4 was lower for both H:CS 70:30 (70%) and CS gels (85%) after 3 h exposure. Here the temperature did not play a major role in regard to the equilibrium swelling ratio. At 37°C the fairly collapsed gels showed only approximately 10% higher swelling. However, with increasing alkalinity riboflavin becomes significantly more soluble. In this case, the higher solubility of riboflavin might have contributed to the still fairly fast release from a far less swollen gel matrix at this pH value (Fig. 7).

The presence of hemicellulose in H:CS 70:30 gels, however, clearly reduced the release rate compared to pure CS gels. In order to interpret the experimental results better, drug release mechanisms were determined by fitting the first 60% of the release profiles into the following equation (Eq. 6, Ritger and Peppas 1987),

$$\frac{M_t}{M_\infty} = kt^n \quad (6)$$

where M_t/M_∞ is the fractional release of drug in time t , k is the constant characteristic of the drug-polymer system, and n is the diffusion exponent characteristic of the release mechanism.

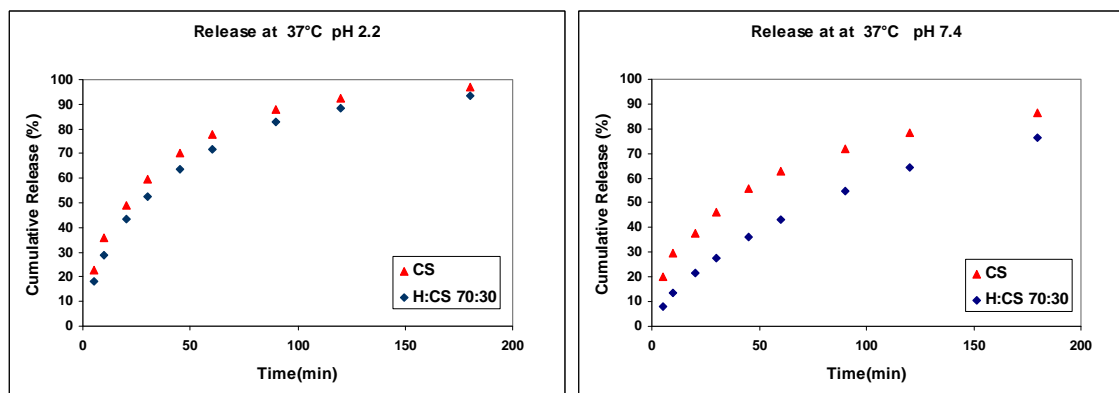


Fig. 8. Release of riboflavin from semi-IPN hydrogels as a function of time in (a) pH 2.2 and (b) pH 7.4 buffer solutions at 37°C.

Table 5. Kinetic Constants (k), Release Exponents (n) and Determination Coefficients (r^2) Obtained from the First 60% of Cumulative Release Data (Eq.6)

Films	n	k	r^2
CS at pH 2.2	0.52	0.101	0.990
CS at pH 7.4	0.45	0.099	0.993
H:CS 70:30 at pH 2.2	0.60	0.070	0.995
H:CS 70:30 at pH 7.4	0.66	0.287	0.998

According to Eq.6, for polymer films, the value of $n=0.5$ implies that the drug release is controlled mostly by diffusion, while swelling- (or chain relaxation) controlled drug release occurs in case of $n=1.0$. The values between 0.5 and 1.0 are indicative of the release behavior being controlled by both phenomena. H:CS 70:30 hydrogels at both pH levels showed non-Fickian behavior ($0.5 < n < 1$), indicating that the drug release was due to both drug diffusion and chain relaxation of the hydrogel matrix (see Table.5). However, n values for CS hydrogels were relatively close to $n=0.5$ (for thin film), suggesting that the release was dominated by Fickian diffusion (Lynch and Dawson 2004; Liu et al. 2010). At pH 7.4 CS gels begin to lose their swelling capacity. It can therefore be argued that n values drop below 0.5, implying a beginning transformation from a gel to a solid material.

Further, equilibrium swelling of the gel matrix was reached after approximately one hour; however, the drug continued to be discharged into the release medium for additional two hours, which is one more indication for the release to follow a combined mechanism of diffusion and chain relaxation.

CONCLUSIONS

1. An innovative alkaline extraction technique was used to separate hemicellulose from low-value aspen biomass. Although the isolated hemicellulose was fairly polydisperse, a sufficiently large amount of polymeric polysaccharides could be preserved.
2. Novel pH-sensitive semi-IPN hydrogels were developed based on the extracted high molecular weight hemicellulose and crosslinked chitosan as a matrix.
3. Crystallites introduced through hemicellulose enhanced the coherence of the swollen semi-IPN hydrogels.
4. It is assumed that although covalent crosslinks predominantly influenced the mechanical stability, fewer and/or longer crosslinks were formed in presence of hemicellulose, thus improving the response to pH-induced swelling. Higher swelling ratios were observed with increasing hemicellulose content.
5. Swelling ratios were high at low pH due to repulsion of the charged groups in the chitosan gel and low at the physiological pH of 7.4. Riboflavin was selected as a model drug due to its low solubility and minimal interference with the gel matrix. An *in vitro* release study of riboflavin showed that these semi-IPNs could have potential for application as pH-sensitive controlled drug delivery vehicles in physiological environments, e.g., for antibiotics or antiulcer drugs in the stomach. At low pH the highly swollen hydrogel matrix would fairly easily discharge the drug, while at higher pH values the gel matrix is collapsed, and the release is dominated by the solubility of the drug in the release medium.

ACKNOWLEDGMENTS

The authors are grateful for the support of the Wood Education and Resource Center, NA Grant. No. 07-DG-11420004-235.

REFERENCES CITED

- Anseth, K. S., Bowman, C. N., and Bannon-Peppas, L., (1996). "Mechanical properties of hydrogels and their experimental determination," *Biomaterials* 17, 1647-1657.
- Berger, J., Reist, M., Mayer, J. M., Felt, O., and Gurny R. (2004). "Structure and interactions in covalently and ionically crosslinked chitosan hydrogels for biomedical applications," *European Journal of Pharmaceutics and Biopharmaceutics* 57, 19-34.
- Coviello, T., Matricardi, P., Marianecchi, C., and Alhaique, F. (2007). "Polysaccharide hydrogels for modified release formulations," *Journal of Controlled Release* 119, 5-24.
- Čulin, J., Šmit, I., Andreis, M., Veksli, Z., Anžlovar, A. and Žigon, M. (2005). "Motional heterogeneity and phase separation of semi-interpenetrating networks and mixtures based on functionalised polyurethane and polymethacrylate prepolymers," *Polymer* 46, 89-99.
- Curotto, E., and Aros, F. (1993). "Quantitative determination of chitosan and the percentage of free amino groups," *Analytical Biochemistry* 211, 240-241.
- Ebringerova, A. (2006). "Structural diversity and application potential of hemicelluloses," *Macromol. Symp.* 232, 1-12.
- Gabriellii, I., and Gatenholm, P. (1998). "Preparation and properties of hydrogels based on hemicellulose," *Journal of Applied Polymer Science* 69, 1661-1667.
- Gabriellii, I., Gatenholm, P., Glasser, W. G., Jain, R. K., and Kenne, L. (2000). "Separation, characterization and hydrogel-formation of hemicellulose from aspen wood," *Carbohydrate Polymers* 43, 367-374.
- Gatenholm, P., and Tenkanen, M. (2004). *Hemicelluloses: Science and technology*, Oxford University Press, 15-16
- Guan, Y. L., Shao, L., and Yao, K. D. (1996). "A study on correlation between water state and swelling kinetics of chitosan-based hydrogels," *Journal of Applied Polymer Science* 61, 2325-2335
- Hansen, N. M. L., and Plackett, D. (2008), "Sustainable films and coatings from hemicelluloses: A review," *Biomacromolecules* 6, 1493-1505
- Hoare, T. R., and Kohane, D. S. (2008). "Hydrogels in drug delivery: Progress and challenges," *Polymer* 49, 1993-2007.
- Jin, S., Liu, M., Zhang, F., Chen, S., and Niu, A. (2006). "Synthesis and characterization of pH-sensitivity semi-IPN hydrogel based on hydrogen bond between poly(N-vinylpyrrolidone) and poly(acrylic acid)," *Polymer* 47, 1526-1532.
- Kumar, M. N. V. R., Muzzarelli, R. A. A., Muzzarelli, C., Sashiwa, H., and Domb, A. J. (2004). "Chitosan chemistry and pharmaceutical perspectives," *Chemical Reviews* 104, 6017-6084.
- Lindblad, M. S., Albertsson, A. C., Ranucci, E., Laus, M., and Giani, E. (2005). "Biodegradable polymers from renewable sources: Rheological characterization of hemicellulose-based hydrogels," *Biomacromolecules* 6, 684-690.
- Lindblad, M. S., Ranucci, E., and Albertsson, A. C., (2001). "Biodegradable polymers from renewable sources. New hemicellulose-based hydrogels," *Macromolecular Rapid Communications* 22, 962-967.

- Liu, C., Chena, Y., and Chena, J. (2010). "Synthesis and characteristics of pH-sensitive semi-interpenetrating polymer network hydrogels based on konjac glucomannan and poly(aspartic acid) for in vitro drug delivery," *Carbohydrate Polymers* 79, 500-506.
- Lou, X., and Copenhagen, C. (2003). "Mechanical characteristics of poly(2-hydroxyethyl methacrylate) hydrogels crosslinked with various difunctional compounds," *Polymer International* 50, 319-325.
- Lynch, I., and Dawson, K. A. (2004). "Release of model compounds from Plum-Pudding-type gels composed of microgel particles randomly dispersed in a gel matrix," *Journal of Physical Chemistry B* 108, 10893-10898.
- Ma, P. X., and Elisseeff, J. H. (2005). *Scaffolding in Tissue Engineering*, CRC Press, Boca Raton.
- Mi, F. L., Tan, Y. C., Liang H.C., Huang R.N. and Sung H.W. (2001). "In vitro evaluation of a chitosan membrane cross-linked with genipin," *Journal of Biomaterials Science Polymer Edition* 12, 835-850.
- Myung, D., Waters, D., Wiseman, M., Duhamel, P. E., Noolandi, J., Ta, C. N., and Frank, C.W. (2008). "Progress in the development of interpenetrating polymer network hydrogels," *Polymers for Advanced Technologies* 19, 647-657.
- Peppas, N. A., Bures, P., Leobandung, W., and Ichikawa, H. (2000). "Hydrogels in pharmaceutical formulations," *European Journal of Pharmaceutics and Biopharmaceutics* 50, 27-46.
- Peppas, N. A., Hilt, J. Z., Khademhosseini, A., and Langer, R. (2006). "Hydrogels in biology and medicine: From molecular principles to bionanotechnology," *Advanced Materials* 18, 1345-1360.
- Ritger, P. L., and Peppas, N. A. (1987). "A simple equation for description of solute release I. Fickian and Non-Fickian release from swellable devices," *Journal of Control Release* 5, 37-42.
- Rogers, K., Etok, S., Broadhurst, A., and Scott, R. (2005). "Enhanced analysis of biomaterials by synchrotron diffraction," *Nuclear Instruments and Methods in Physics Research Section A: Accelerators, Spectrometers, Detectors and Associated Equipment* 548, pp.123-128.
- Schexnailder P. and Schmidt G. (2009). "Nanocomposite polymer hydrogels", *Colloid and Polymer Science* 287, 1-11.
- Shu, X. Z., Zhu, K. J., and Song, W. (2001). "Novel pH-sensitive citrate cross-linked chitosan film for drug controlled release," *International Journal of Pharmaceutics* 212, 19-28.
- Slaughter, B. V., Khurshid, S. S., Fisher, O. Z., Khademhosseini, A., and Peppas, N. A. (2009). "Hydrogels in regenerative medicine," *Advanced Materials* 21, 1-23.
- Tanaka, Y., Gong, J. P., and Osada, Y. (2005). "Novel hydrogels with excellent mechanical performance," *Progress in Polymer Science* 30, 1-9.
- Teleman, A., Lundqvist, J., Tjerneld, F., Stalbrand, H., and Dahlman, O. (2000). "Characterization of acetylated 4-O-methylglucuronoxylan isolated from aspen employing H- and C-NMR spectroscopy," *Carbohydrate Research* 329, 807-815.
- Timell, T.E. (1967). "Recent progress in the chemistry of wood hemicelluloses," *Wood Science and Technology* 1, 45-70.

- Yu, H., Lu, J., and Xia, C. (2007). "Preparation and properties of novel hydrogels from oxidized konjac glucomannan cross-linked chitosan for in vitro drug delivery," *Macromolecular Bioscience* 7, 1100-1111.
- Yui, N. (2002). *Supramolecular Design for Biological Applications*, CRC Press, Boca Raton.
- Zhang, G. Q., Zha, L. S., Zhou, M. H., Ma, J. H., and Liang, B. R. (2005). "Preparation and characterization of pH- and temperature- responsive semi-interpenetrating polymer network hydrogels based on linear sodium alginate and crosslinked poly(N-isopropylacrylamide)," *Journal of Applied Polymer Science* 97, 1931-1940.
- Zhao, Y., Kang, J., and Tan, T. W. (2006). "Salt-, pH- and temperature-responsive semi-interpenetrating polymer network hydrogel based on poly(aspartic acid) and poly(acrylic acid)," *Polymer* 47, 7702-7710.
- Zugic, D., Spasojevic, P., Petrovic, Z., and Djonlagic, J. (2009). "Semi-interpenetrating networks based on poly(N-isopropyl acrylamide) and poly(N-vinylpyrrolidone)," *Journal of Applied Polymer Science* 113, 1593-1603.

Article originally submitted: Feb.17, 2010; Peer review completed: March 11, 2010;
Revised version received, accepted, and published: April 7, 2010.